A THEORETICAL METHOD FOR THE PREDICTION OF UNDERWATER EXPLOSION PULSES AT CAUSTICS

by

I.M. Blatstein
(read by R.M. Barash)

Naval Ordnance Laboratory
White Oak, Silver Spring, Maryland, U.S.

Our concern [Refs. 1 and 2] is with the effect of refraction on the long range propagation of underwater explosion shock waves. Here, as with acoustic sources, ray tracing can be used to predict refraction effects. From the divergence or convergence of rays, an amplification factor can be calculated. This is defined as the square root of the ratio of the cross sectional area between rays at a given point assuming spherical spreading to the cross sectional area between rays at the same point when the actual sound velocity profile is specified. We can then multiply the pressure history expected at a given point if no refraction occurred by the appropriate amplification factor. This then gives us the pressure history expected at that point when refraction is accounted for.

However, the amplification factor is inversely proportional to the square root of the cross sectional area between adjacent rays. So as we approach a caustic, where these rays cross, the amplification factor reaches infinity, and ray theory is invalid. Furthermore, in the shadow zone adjacent to the caustic, ray theory predicts zero energy penetration. This is due to the high frequency nature of the ray theory approximation. So if we are interested in the pressure near a caustic or in an adjacent shadow zone a method other than ray theory must be used.

In this paper, I will describe such a method for calculating shock wave pressure histories in and near caustic regions. This method involves the incorporation of various propagation effects into a Fourier series representation of the initial shock wave from an underwater explosion. I will then describe comparisons that have been made between calculated pressure histories and experimental results from ocean and flooded quarry tests. Figure 1 shows a typical ray diagram for the ocean case which we have considered. Here the source explosion is at a depth of 1000 ft. The convergence zone caustic then occurs at 20 mi to 30 mi from the source. If the source is deeper, in or just below the thermocline, a thermocline related caustic occurs. This shows up at 2 mi to 5 mi and is due to upward starting rays. The flooded quarry test that we have considered was intended to model this thermocline related caustic. For both cases, comparisons will be shown, agreement will be praised, and discrepancies will be sullenly discussed. Finally, I will talk about the accuracy of ray theory near the caustic, a region where it is known to break down.

A starting point for our work was a solution to the wave equation that has been done at various times in slightly different forms by Brekohvskikh [Ref. 3], Tolstoy [Ref. 4], and in this case, Sachs and Silbiger [Ref. 5], [Fig. 2]. The wave equation is solved for a harmonic source and an arbitrary depth dependent sound velocity profile. First they arrive at a ray solution, where each term in the sum corresponds to an arrival reaching the point of interest after leaving the source at a different initial angle. But as with any ray solution, this one breaks down on the caustic. So they do a further approximation and arrive at an expression valid at and near a caustic for a sinusoidal acoustic source. If we divide this expression by the pressure expected at that point assuming spherical spreading, we get an amplification factor valid at a caustic [Fig. 3].

Most of the quantities in the amplification factor are constants of the propagation path. These are determined once the sound velocity

profile, source depth, and point of interest are given. The expression also contains the Airy function, a function of both frequency through $k^{2/3}$ and distance off the caustic through Δr. For a given source frequency, the Airy function, and so the amplification factor, falls off exponentially as we move to the left of the caustic into the shadow zone. As we start moving to the right of the caustic, which is located at $\Delta r = 0$, the amplification factor at first increases. Further to the right we see an oscillating function. This is the result of two arrivals interfering in what is familiar to us in ray theory as the double arrival region. From an asymptotic expression for the Airy function, it can be shown that one arrival is approaching the caustic and has been amplified. The other arrival is receding from the caustic. It has been amplified and also phase shifted by 90°. While this information about phase shifts and amplitudes is difficult to verify in the resultant signal from a sinusoidal source, it is more readily seen in the resultant signal from a transient such as a shock wave. We will see this in some of the figures.

Now that we have a frequency dependent amplification factor, we need to apply it to a shock wave. Our next step is to describe the shock wave in a frequency dependent manner. This has to be done in such a way that we describe what the shock wave would look like at the range of the caustic if no refraction occurred. Then we can incorporate our amplification factor into the pressure history in order to account for refraction.

We represent the initial shock wave as an abrupt rise to a peak pressure followed by an exponential decay [Fig. 4]. We then write the Fourier series for the pulse. This way it is expressed in a frequency dependent manner. In this figure, the amplitude of the shock wave is normalized to one. In general, we will need both a peak pressure, P_1, and a decay constant, θ, to determine the pulse shape and series. We would like these parameters to be characteristic of the range of interest and also to take into account the finite amplitude effects that are present in the propagation of a shock wave.

We do this by using the similitude, or scaling, equations which were discussed in the companion paper by Barash and Goertner [Ref. 6] (see Sect. 3 of these Proceedings). Since these equations are based on cube root scaling, they properly account for the finite amplitude effects on the peak pressure and decay constant. However, they have not been verified out to the 30 mi range at which we need P_1 and θ. So we use them to a range where they are known to be valid, and the peak pressure is low enough so that we may ignore finite amplitude effects beyond that range. The point at which we cease to account for finite amplitude effects is the range at which the peak pressure drops below 5 psi. From this point to the range of the caustic we assume acoustic spherical spreading to find P_1 and θ for our pulse.

We now have the shock wave in a frequency dependent form with the appropriate peak pressure and θ. The next step is to incorporate our amplification factor into the expression [Fig. 5].

The expression at the top of the figure is the Fourier series for the pressure history with refraction added. P_1 and θ are the pulse parameters we have just discussed. The function represented by the script f_p to the right of the summation sign is the refractive amplification factor. This along with the $\pi/4$ added to the arguments of the sine and cosine take into account the effect of refraction on the propagating pulse near the caustic. This new expression, if evaluated as it stands, would diverge. The physically unrealizable step discontinuity in the pulse would lead to an infinite spike when refraction was added. However, we have yet to take into account the attenuation of acoustic pressure disturbances that becomes important for long ranges and high frequencies. Not only is it an important effect over the long propagation path to the caustic, but it serves to force our series to converge and terminate at some finite frequency. The graph in the centre of this figure shows the relative strength as a function of wave number, k, of the refraction factor f, and an absorption factor β. We can see that the ocean acts as a filter, damping the high frequency components

of the shock wave. Thus by adding absorption, we get the expression at the bottom of this figure for the pressure near a caustic. It is a Fourier series that now terminates at some finite frequency due to absorption. This limitation shows up as the summation now only extends to N rather than infinity. Once we find the range to the caustic for the depth of interest, and determine the absorption cut-off, N, the expression for the pressure may be thought of as being purely a function of Δr, the distance off the caustic. The next figures show pulses calculated for various Δr's, along with experimental pressure histories from the convergence zone experiment we treated [Fig. 6a]. The pulse on the right is a typical experimental record. Those on the left are calculated. For negative Δr, we are in the shadow zone. Here we see a broad, low amplitude pulse. This is a result of the action of the Airy function, which is monotonically decreasing with frequency in this region. In the caustic region [Fig. 6b], we observe a single arrival with a high amplitude and short decay time. As we move away from the caustic, the peak pressure at first grows and then starts to decrease. Also shown in the figure is the isovelocity pressure history. This is what the pressure history would look like at the range of the caustic if no refraction occurred. For larger distances off the caustic [Fig. 6c], there are two arrivals, the resultant of the two arrivals from various frequencies. The first has just been amplified and has approximately the same decay constant as the isovelocity pressure history. The second arrival has been amplified and further phase-shifted by 90°. This phase shift leads to a much shorter decay constant as seen in the figure. Thus, for a shock wave, the effect of the phase shift shows up clearly.

At this point, I have described the method for calculations near a caustic and shown qualitatively what to expect. Next, I will show the comparisons of calculated pressure histories and experimental results that have been made.

The first such comparison involves an oceanic experiment done by the Naval Ordnance Laboratory.

The purpose of this experiment was to record pressure histories in a convergence zone. Figure 1 showed an average sound velocity profile and associated ray diagram for the time period of the experiment. During the experiment, one ship set off charges of 8 lb and 900 lb of TNT in a region from near the surface to 1000 ft deep. Another ship some 30 mi away used a vertical array of more than 100 hydrophones to record pressure histories throughout the convergence zone. When the gauge array was placed so that it crossed the caustic for a given shot, pressure histories were then obtained for the shadow zone, caustic region, and double arrival region, simultaneously.

We selected five of these shots to test the method just described. We will show representative pressure histories from four of these shots.

In order to do the calculations, we must know the depth of the gauge string with respect to the caustic. For these shots, this was determined from an analysis of the experimental pressure histories. In Fig.7, the position of the gauge string for each shot is indicated on an enlarged view of the upper region of the convergence zone. We notice that there is a reflected branch of the caustic resulting from surface reflection, as well as the direct branch. Gauges at various positions will record different pressure histories due to their proximity to both branches of the caustic. For the first two shots considered, due to lack of complete data, we will only consider the contribution from the direct caustic.

We will first consider shot 151 [Fig. 8], an 8 lb shot where the gauge string was relatively deep. For shot 151, we first specify the gauge of interest, for example, the gauge near the top of the gauge string. Then we calculate the parameters needed for the amplification factor on the caustic at that depth using the given sound velocity profile and source depth. Then from this figure we determine Δr, the horizontal distance from the gauge to the caustic, and the final parameter needed.

Figure 8 contains this calculated pressure history, and the experimental record from this gauge in the shadow zone in the upper left-hand corner. Next to it is a comparison in the caustic region, and at the bottom of the slide are two comparisons in the double arrival region. In all cases the experimental record is a solid line, while the calculated record is a dashed line. In all three regions, the calculated pressure histories adequately match the experimental records. In the upper right-hand corner we have also plotted the isovelocity pressure history. This again is what the pressure history would look like at all four gauges at the range of the caustic if no refraction occurred.

Also of interest is the good agreement for relatively long times after the peak pressure. The caustic solution used in our pressure history retains some of the high frequency limitations of ray theory. This would suggest that for each arrival we could only make valid predictions near the peak pressure where high frequencies predominate. Yet these calculations yield good results beyond the point where the pressure history drops below zero and flattens out. This indicates a reasonably good description of the low frequency content of the pulse. This is probably due to the relatively small sound velocity gradients in the ocean which make the caustic solution valid for relatively low frequencies on the order of 100 Hz or less. This low frequency validity should extend to ray theory as well, despite the often made remark that ray theory is valid for high frequencies only.

The next shot we consider is shot 82 [Fig. 9], an 890 lb explosion at 1000 ft. The same general agreement between experimental records and calculated pressure histories is evident. In the records closest to the caustic, [Figs. 9b & 9c], gauge case ringing is very severe and interferes somewhat with the comparisons.

Now we will consider the two shots where both the direct and reflected arrivals were recorded. A gauge at the bottom of the gauge string for shot 120 is in the double arrival region of the direct branch caustic and in the shadow zone of the reflected branch caustic.

Hence, we would expect arrivals due to both branches. From ray geometry we can calculate the arrival time difference, or time delay, between these arrivals from different branches. We further assume that the surface acts as a perfect reflector for the reflected arrivals, causing only a phase reversal. We then combine the resulting pulses with the appropriate time delay to find the pressure history.

Figure 10 shows comparisons of these calculated pressure histories and experimental records from the top, middle, and bottom of the gauge string. In the bottom record, the pressure history starts with a direct double arrival, which is then followed by a negative shadow zone pulse from the reflected caustic. Again the general agreement of peak pressure and wave forms is good.

As the last of the oceanic comparisons, we calculated pressure histories for shot 119, an 8 lb shot [Fig. 11]. This differed from the previous shot in that it is a smaller charge weight, and so we are dealing with pulses with a much shorter decay time. This means there is proportionately more high frequency energy. By treating records with reflected arrivals in them, we are able to test the method for considerable distances off the caustic. in Fig. 11, the reflected arrival is approximately 1600 ft horizontally into the shadow zone, and the direct double arrival is approximately 2400 ft horizontally from the direct caustic. So with one record we gain information about a region 4000 ft wide.

In all four comparisons, the calculated pressures are in reasonable agreement with the experimental values from the oceanic test. Just as important, the entire waveforms are in good agreement. So for the oceanic convergence zone case, the method is a reasonable approximation for the various phenomena involved in propagation to a convergence zone.

We also tried matching pressure records from a test conducted by Woods Hole in a flooded quarry [Fig. 12]. As I have said, this type

of test models the thermocline related caustic that may occur at 2 mi to 5 mi. For the quarry case the solution to the wave equation is not clearly valid for the frequency domain of our pulse. Not only are the sound velocity gradients 1000 times larger in the quarry than in the ocean, but the caustic is much closer to the turning points of the rays. This could tend to restrict the validity to the higher frequencies in the pulse.

Also, we have to modify the pressure expression since absorption is no longer the high frequency cut-off mechanism as it was in the ocean. Here the gauge response restricts high frequencies more than absorption, so the gauge response as a function of frequency is used in the pressure expression instead of absorption.

Pressure histories were then calculated near the caustic and in the double arrival region for a 56 lb charge detonated at 50 ft [Fig. 13]. The dashed lines are the calculated pulses, the solid lines are the experimental pressure records. While the exact agreement of the peak pressures is no doubt fortuitous, good agreement between experimental and calculated peak pressures has been obtained for similar quarry data during the course of this analysis. However, it is also apparent from this figure that the decay from the peak pressure is much too steep.

If the solution to the wave equation is indeed valid only for high frequencies for this case, it may explain why our calculations only appear reasonable near the peak pressure where high frequencies predominate. Also, it is possible that a propagation mode other than the pure refracted one contributes to the pressure at a thermocline related caustic. For example, a lateral wave type of propagation could be occurring at the interface of the almost-isovelocity upper layer in the flooded quarry. This would be energy at relatively low frequencies which would affect most the decay from the peak. Or it is possible that the surface boundary is influencing the propagation of energy in a way not accounted for by ordinary ray theory. If this

were the case, a modified ray theory such as that described by Murphy and Davis in these Proceedings might be necessary for this type of situation. Whatever the reason, the calculation of the decay of the pulse for the quarry case remains the aspect of this work that requires the most improvement.

Finally, I would like to discuss the validity of ray theory near the caustic. Qualitatively we know that ray theory predicts an increasing intensity as one approaches the caustic from the double arrival region. This intensity, which is the same for all frequencies, reaches infinity on the caustic, a line of zero width. The caustic solution that we are using yields a different picture. For this solution, the caustic is a region of finite thickness in between the shadow zone and double arrival region. The lower the frequency of the source, or the larger the charge for the transient case, the wider the caustic region is. Inside the caustic region, the solution yields one arrival that slowly increases in amplitude as one moves away from the shadow zone boundary at $\Delta r = 0$. For large distances off the caustic, the expression yields two arrivals in the pressure history. This is the double arrival region as expected from ray theory. However, since the caustic solution was derived to be valid near the caustic, it is not obvious that it should yield reasonable results far from the caustic in the double arrival region. So really there are two questions to be answered: How different are ray theory and the caustic solution in the caustic region where ray theory is supposed to be breaking down? and How do ray theory and the caustic solution compare in the double arrival region, where the caustic solution was not originally intended for use?

Referring to Fig. 14, for reasons of simplicity, calculations were done for a harmonic source rather than the pulse sources we have been treating. For the figure we have assumed a 100 Hz harmonic source and the convergence zone sound velocity profile previously shown. In the caustic region, we have combined the two ray arrivals in order to compare the resultant to the caustic solution we have

been using. As expected, as we approach the caustic, the two solutions diverge as the ray solution increases rapidly. It should be remembered that this figure holds true for the particular convergence zone profile treated. We have examined others where the caustic region was narrower, and some where the caustic region was up to three times as wide as this one is. Also shown in the figure is the double arrival region. Here we can resolve two arrivals in the caustic solution. It turns out that each one has the same amplitude, which falls off as the fourth root of Δr. We have plotted this amplitude along with those of the two ray arrivals. If we combined the caustic solution arrivals at the caustic region boundary, the resultant would match the caustic region solution at the caustic region boundary. However, what is most striking is the agreement between ray theory and the caustic solution far into the double arrival region. This explains why our calculations of pulses in the double arrival region were in good agreement with the experimental pulses. While in the double arrival region, one would tend to trust ray theory more, this figure indicates that it is not a bad approximation to continue using the caustic solution that was used in the shadow zone and caustic region.

In order to put all of these results in their proper perspective, we must keep in mind the assumptions and approximations made. We assumed that the unrefracted shock wave could be approximated by an abrupt rise followed by an exponential decay. We then wrote the Fourier series for this pulse. In the oceanic case, we assumed that a superposition of finite amplitude effects, spherical spreading, and absorption on this series would adequately describe long distance propagation in the absence of refraction. Then we added refraction effects to find the pressure near a caustic. In the quarry, the gauge response was substituted for absorption. Our ability to apply these effects separately is no doubt due to the phenomena being treated. Finite amplitude effects occur relatively close in where pressures are high. Absorption for high frequencies takes effect only over long distances. While refraction effects occur throughout the path, the major effect is the significant amplification at the convergence zone. So while these effects no doubt interfere, their major influence is individual.

The main thrust of this work has been to describe the effect of refraction on the propagation of an underwater explosion shock wave. Particularly, we are interested in calculations near the caustic where the refractive amplification is greatest. We feel that in this method we have a reasonable means of calculating just such pressure histories for the oceanic convergence zone. What I also hope has been demonstrated by this paper, and the companion one by Barash and Goertner [Ref. 6], is that an underwater explosion can be more than just a source of energy at various frequencies for acousticians interested in harmonic sources. These transient sources can also lead to analyses and information about ray theory validity that would be otherwise difficult to obtain.

REFERENCES

1. I.M. Blatstein, "Calculations of Underwater Explosion Pulses at Caustics", J. Acoust. Soc. Am., Vol. 49, p. 1568, 1971.

2. I.M. Blatstein, "Refraction of Underwater Explosion Shock Waves: Calculations of Pressure Histories in a Convergence Zone", NOLTR 71-93, Naval Ordnance Laboratory, 1971.

3. L.M. Brekovskikh, "Waves in Layered Media", Academic, New York, Ch. 6, 1960.

4. I. Tolstoy and C.S. Clay, "Ocean Acoustics", McGraw-Hill, New York, Ch. 2, 1966.

5. D. Sachs and A. Silbiger, "The Focusing of Harmonic Sound and Transient Pulses in Stratified Media", J. Acoust. Soc. Am., Vol. 49, pp 824-840, 1971.

6. R.M. Barash and J.A. Goertner, "Experimental Data on the Refraction of Underwater Explosion Pulses". Paper presented at Conference on Geometrical Acoustics at SACLANT ASW Research Centre, La Spezia, Italy, 27-30 Sept 1971.

7. R.R. Brockhurst, J.G. Bruce and A.B. Arons, "Refraction of Underwater Explosion Shock Waves by a Strong Velocity Gradient", J. Acoust. Soc. Am., Vol. 33, No. 4, pp 452-456, 1961.

DISCUSSION

During the discussion the points were made that in a sense one was "saved by absorption", that taking more terms in the Fourier series expansion would not help, and that the use of a mix of linear and non-linear properties, although expedient, may not be valid at large distances.

SOUND VELOCITY PROFILE AND RAY DIAGRAM FOR A CONVERGENCE ZONE CAUSTIC

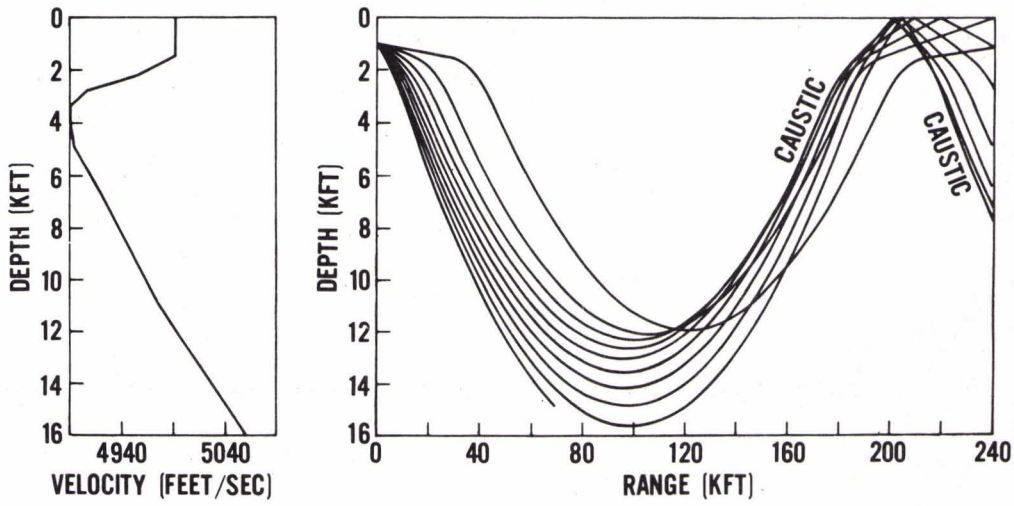

FIG. 1

SAMPLE VELOCITY PROFILE AND RAY DIAGRAM INDICATING WAVE EQUATION SOLUTION PARMETERS (AFTER SILBIGER)

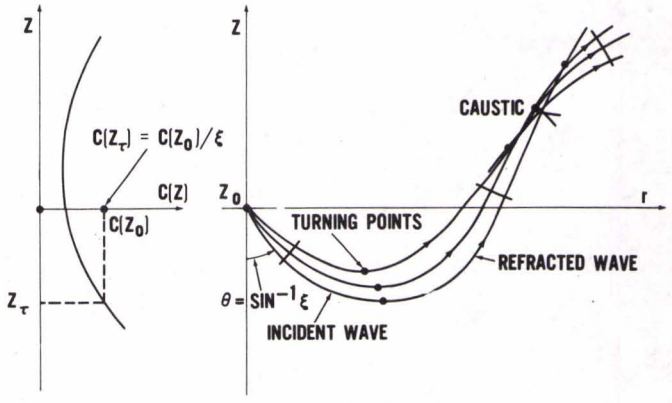

FIG. 2

SOURCE: $P_S = P_0 \cos(wt)$

WAVE EQTN: $\nabla^2 P + K^2 n^2(Z) P = P_0 \delta(x)\delta(y)\delta(z)$

SOLUTION FOR PRESSURE IN THE CAUSTIC REGION:

$$P(r, Zc) = \frac{P_0}{4\pi} K^{1/6} \zeta \left[\frac{2\pi\xi_c}{r_c (n^2(Z) - \xi_c^2)^{1/2} (1-\xi_c^2)^{1/2}} \right]^{1/2} Ai(\pm K^{2/3} \zeta \Delta r) e^{iKW_c - i\pi/4}$$

AMPLIFICATION FACTOR

$$f_p(k, \Delta r) = Rk^{1/6}\,\zeta\left[\frac{2\pi\xi_c}{r_c(n^2-\xi_c^2)^{1/2}(1-\xi_c^2)^{1/2}}\right]^{1/2} \mathrm{Ai}(\pm k^{2/3}\,\zeta\Delta r)$$

where $\mathrm{Ai}(\pm\rho)$ for $W'''_c \leq 0$

FIG. 3

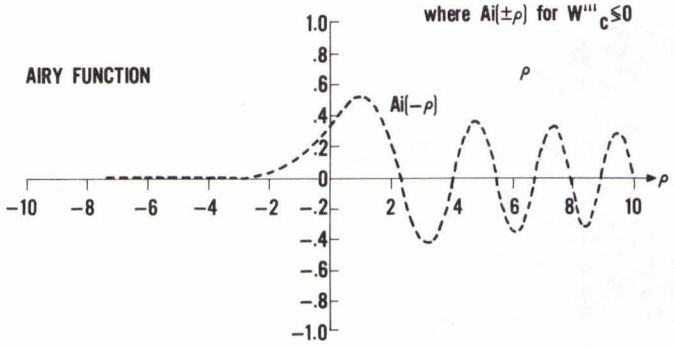

THE REGION OF DEFINITION FOR THE EXPONENTIAL DECAY REPRESENTED BY A FOURIER SERIES

SIMILITUDE EQUATIONS

$P_s(R,W) = 2.16 \times 10^4 (W^{1/3}/R)^{1.13}$ (PSI)

$\theta_s(R,W) = .06W^{1/3}\,(W^{1/3}/R)^{-.22}$ (MSEC)

R IS IN FEET, W IS IN LBS.

$P(t) = 0 \quad -C<t<0$

$P(t) = e^{-t/\theta} \quad 0\leq t\leq C$

FIG. 4

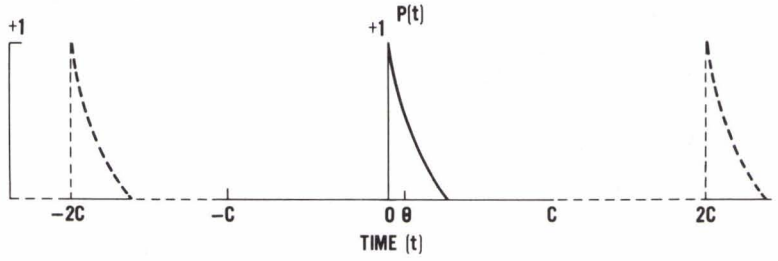

PRESSURE HISTORY WITH REFRACTION

$$P_a(t) = P_1\left(B_0 + \sum_{q=1}^{\infty} f_p(k,\Delta r)B(q) \cdot\left[\frac{a}{\theta}\cos\left(\frac{q\pi t}{a}+\frac{\pi}{4}\right)+q\pi\sin\left(\frac{q\pi t}{a}+\frac{\pi}{4}\right)\right]\right),$$

WHERE $B(q)=\left[\frac{\theta^2}{a^2+(q\pi\theta)^2}\right]\left[1-(-1)^q e^{-\frac{a}{\theta}}\right]$

FIG. 5

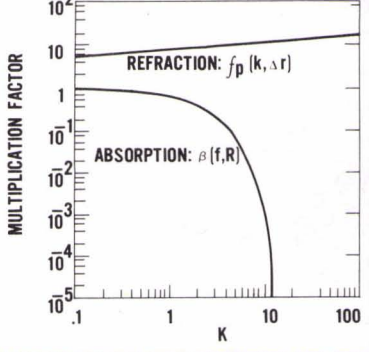

PRESSURE HISTORY WITH REFRACTION AND ABSORPTION:

$$P_r(t) = P_1\left\{B_0+\sum_{q=1}^{N} f_p(k,\Delta r)\beta(f,R_1)B(q) \cdot\left[\frac{a}{\theta}\cos\left(\frac{q\pi t}{a}+\frac{\pi}{4}\right)+q\pi\sin\left(\frac{q\pi t}{a}+\frac{\pi}{4}\right)\right]\right\},$$

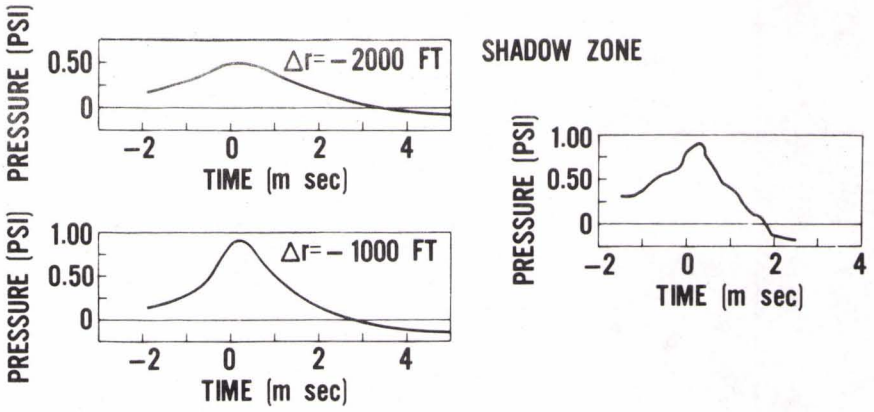

FIG. 6a

EXAMPLES OF PRESSURE-TIME HISTORIES FOR VARIOUS HORIZONTAL DISTANCES FROM A CONVERGENCE ZONE CAUSTIC

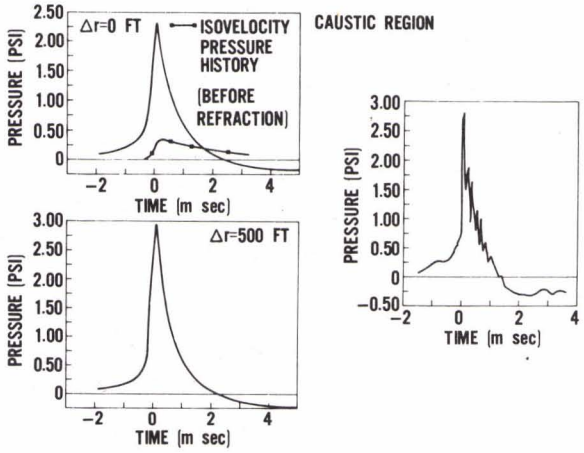

FIG. 6b

EXAMPLES OF PRESSURE-TIME HISTORIES FOR VARIOUS HORIZONTAL DISTANCES FROM A CONVERGENCE ZONE CAUSTIC

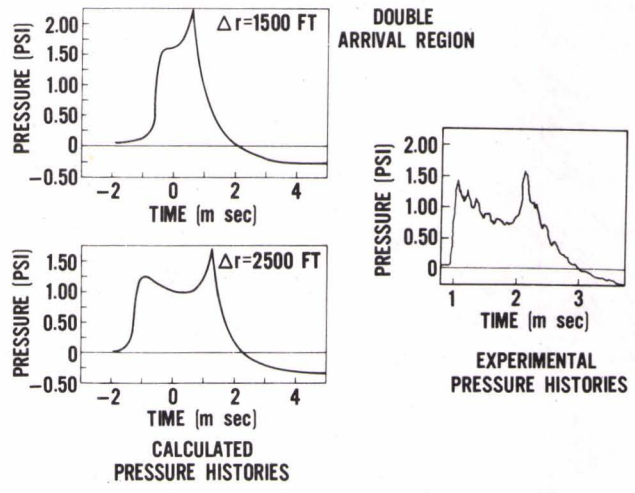

FIG. 6c

EXAMPLES OF PRESSURE-TIME HISTORIES FOR VARIOUS HORIZONTAL DISTANCES FROM A CONVERGENCE ZONE CAUSTIC

FIG. 7

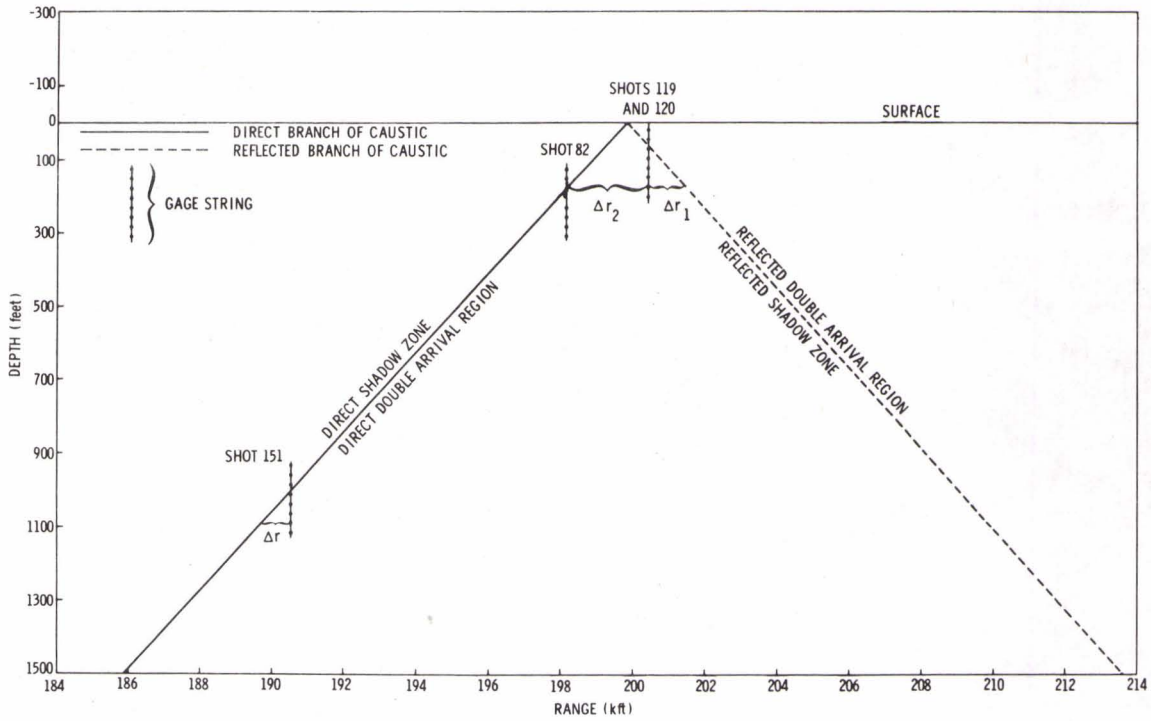

THE POSITION OF THE GAGE STRING WITH RESPECT TO THE CAUSTIC FOR SAMPLE SHOTS

SHOT 151, W = 8LB., COMPARISON OF DATA AND CALCULATED PRESSURE HISTORIES. (A) Z_g = 934 FT. (DEPTH OF GAGE), Δr = −534 FT.; (B) Z_g = 1029 FT., Δr = 379 FT (C) Z_g = 1074 FT., Δr = 802 FT.; (D) Z_g = 1110 FT., Δr = 1152 FT.

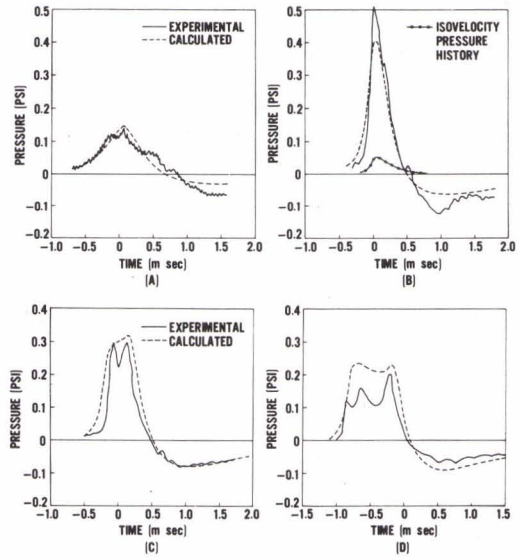

FIG. 8

SHOT 82, W = 890 LB. COMPARISON OF DATA AND CALCULATED PRESSURE HISTORIES. (A) Z_g = 174 FT., Δr = 0 FT.; (B) Z_g = 221 FT., Δr = 383 FT.; (C) Z_g = 235 FT., Δr = 498 FT., (D) Z_g = 320 FT., Δr = 1191 FT.

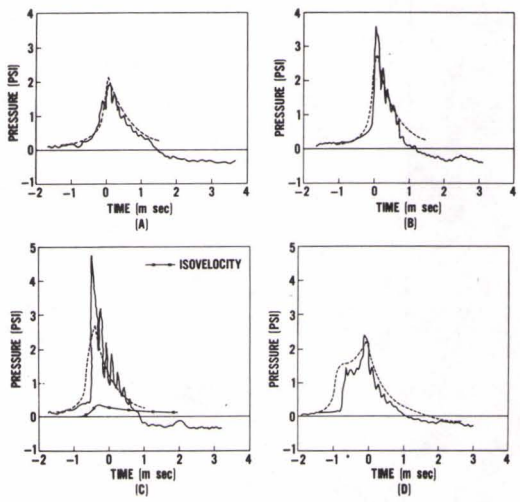

FIG. 9

SHOT 120, W=870 LB. COMPARISON OF DATA AND CALCULATED PRESSURE HISTORIES.
(A) Z_g = 44FT., Δr_2 = 604FT.; Δr_1 = −91FT.; (B) Z_g = 121FT., Δr_2 = 1219FT.
Δr_1 = −693FT.; (C) Z_g = 202FT., Δr_2 = 1861FT., Δr_1 = −1565FT.

FIG. 10

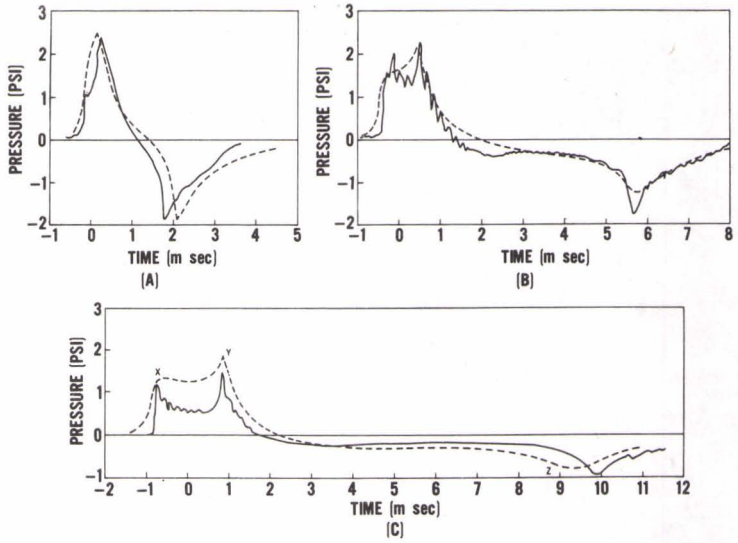

SHOT 119, W=8 LB. COMPARISON OF DATA AND CALCULATED PRESSURE HISTORIES.
(A) Z_g=2 FT., Δr_2=428 FT., Δr_1=380 FT.; (B) Z_g=59 FT., Δr_2=1062 FT.,
Δr_1=−254 FT.; (C) Z_g=202 FT., Δr_2=2365 FT., Δr_1=−1565 FT.

FIG. 11

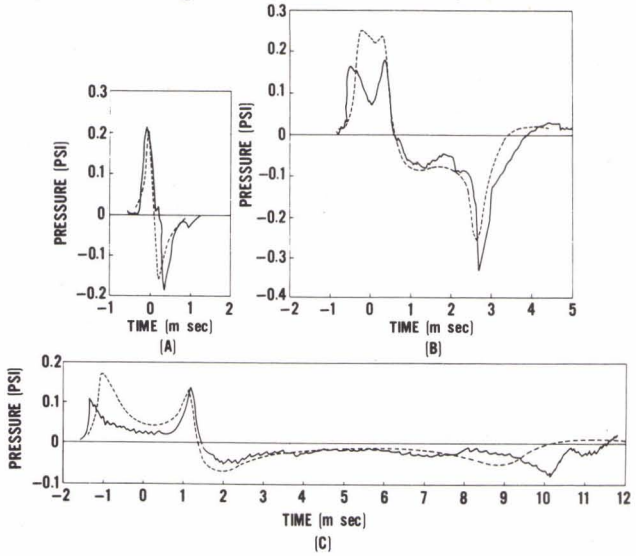

VELOCITY PROFILE AND RAY DIAGRAM FROM BLACKINGTON FARM QUARRY FOR DAY OF WHOI CASE #45

FIG. 12

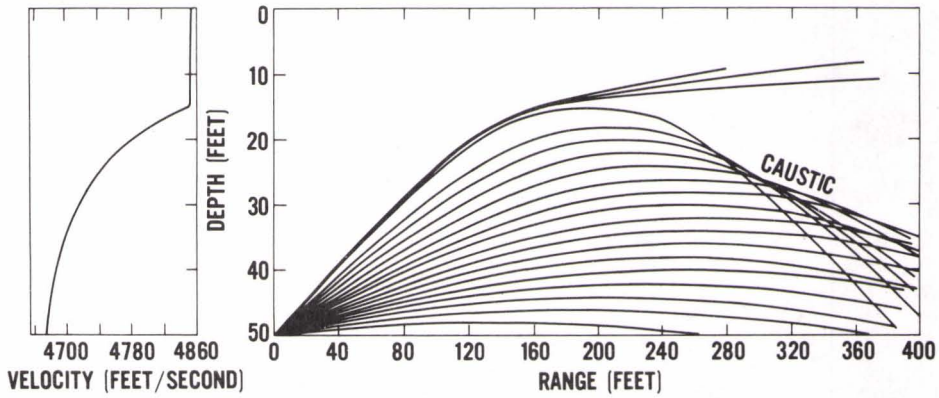

WHOI QUARRY CASE NO. 45, COMPARISON OF DATA AND CALCULATED PRESSURE HISTORIES

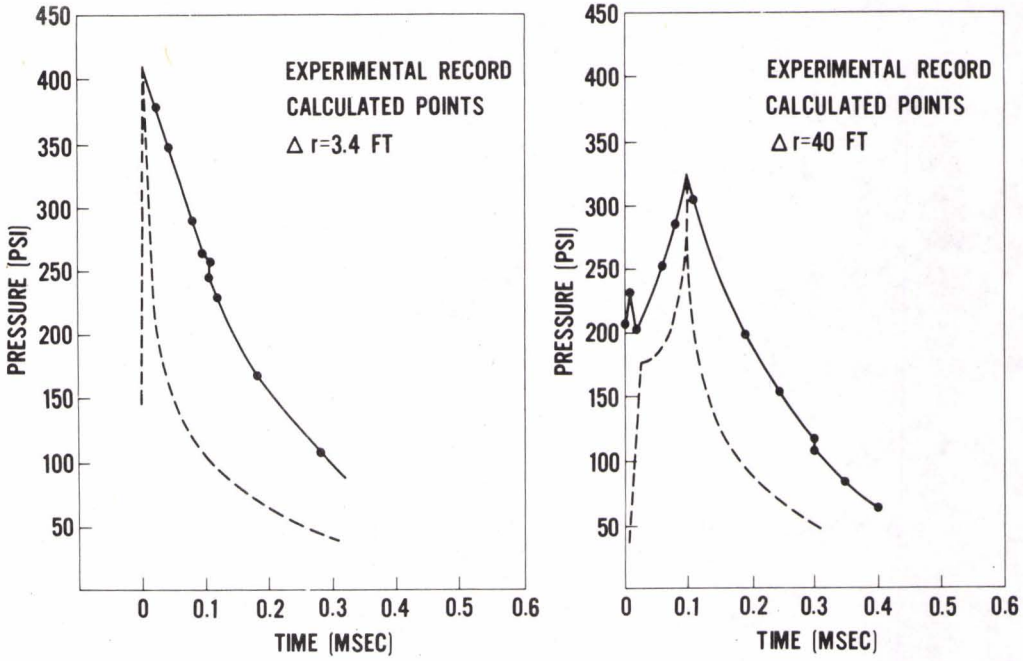

FIG. 13

COMPARISON OF RAY THEORY AND CAUSTIC SOLUTION FOR 100 Hz

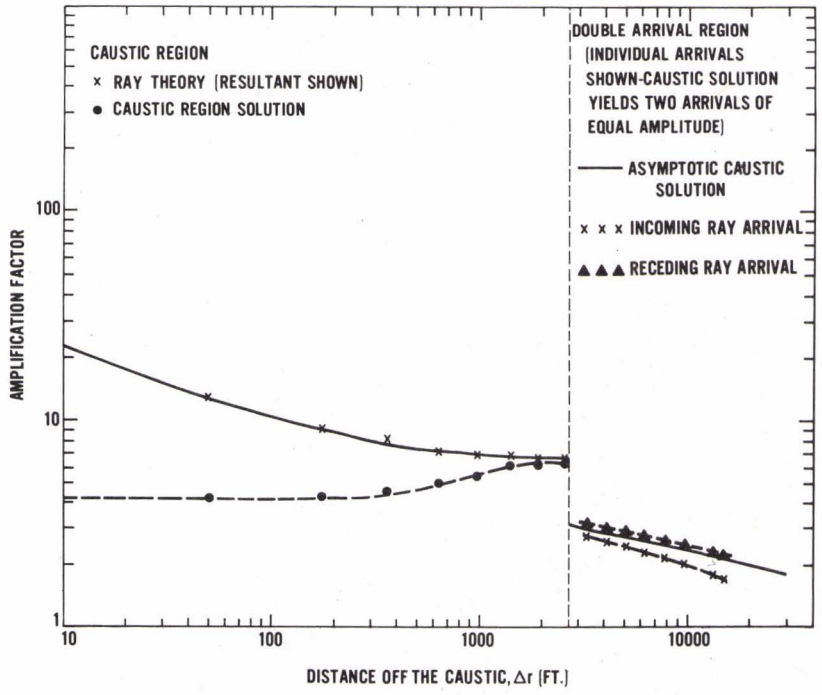

FIG. 14